21st Australasian Fluid Mechanics Conference
Adelaide, Australia
10-13 December 2018

Two Way Coupled Hypersonic Fluid Structure Interaction Simulations with Eilmer

I. H. J. Jahn[1], G. M. D. Currao[2], A. J. Neely[2], R. Gollan[1], P. Jacobs[1]

[1]School of Mechanical and Mining Engineering,
The University of Queensland, St Lucia, Queensland 4072, Australia

[2]School of Engineering and Information Technology
UNSW Canberra at the Australian Defence Force Academy, Canberra, Australian Capital Territory 2612, Australia

Abstract

Fluid Structure Interactions (FSI), if not managed appropriately are known to have contributed to the loss of several aerospace vehicles. As done for the X-43, FSI can be designed-out by making structures sufficiently rigid and by providing appropriate damping. In hypersonic cruise vehicles, this strategy is not applicable as stringent weight limits and large thermal loads result in structures with reduced stiffness [12]. Thus, the accurate simulation and prediction of FSI are essential to allow for the most effective design. In hypersonics, aeroelastic effects can result in rapid variations in pressure and thermal evolutions. The level of coupling between fluid and structure is typically is strong or *two-way*, which means that CFD and FEM solvers have to continuously exchange information in terms of nodal forces and displacement in order to produce an accurate solution. In this paper we present details of a *fast* implementation and first results of a FEM solver in the Eilmer CFD solver. Details are provided on the formulation of the structural solver, the fluid solver to appropriately account for the deforming boundaries, and the coupling approach. The results show that the simulations are in broad agreement with experimental data, but that an off-set exists in response frequency and amplitude. The resulting capability, with its ability to conduct time–accurate FSI simulations is a good tool to further investigate the underlying effects driving hypersonic FSI.

Introduction

The last decade has seen significant advances in sustained hypersonic flight technologies through joint international programs, such as HiFiRE [2], and technological demonstrators, such as the X-51 born from the joint efforts of Boeing and AFRL. These flight programs have been highly successful in demonstrating the feasibility of air-breathing atmospheric flight and increasing the Technology Readiness Level (TRL) of hypersonic systems.

However, the inherent high cost of the flight programs have motivated the development and implementation of numerical methods to support the design and evaluation of vehicle concepts. FSI represents a major threat in the context of vehicle life predictions, as it often implies fatigue, vibration and change in the aerodynamic characteristics. An overview of hypersonic FSI is provided by McNamara *et al.* [12]. Furthermore, Zuchowski [21] provides an overview on the current status of predictive capabilities for hypersonic cruise vehicles.

The last five years have seen an increase in fundamental studies to analyse hypersonic FSI, with numerical and experimental studies conducted specifically to identify the mechanisms by which the fluid, boundary layer, and structures interact [17, 16, 5, 6]. Currao *et al.* have shown that the problem cannot be treated as quasi-steady and that due consideration has to be given to the interaction between the global shape and the boundary layer. Experiments have served well in providing a validation data for FSI and giving an understanding of the process at a macroscopic level. However, to probe the exact mechanisms of excitation and energy exchange, accurate numerical methods are desirable.

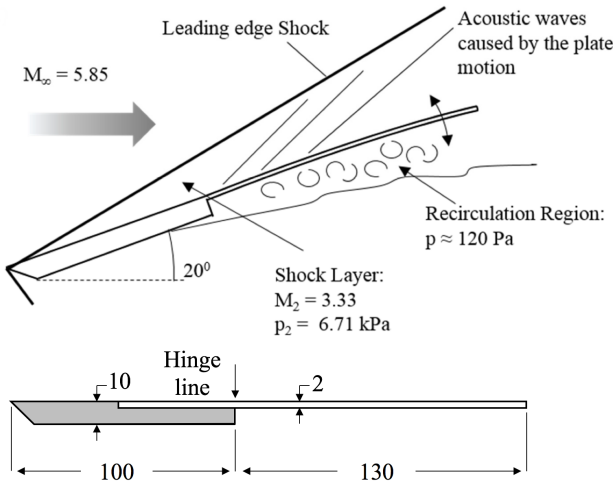

Figure 1: Geometry of the model.

The CFD code Eilmer [8, 9], has been developed within the Centre for Hypersonics at the University of Queensland to provide time–accurate simulation of flows in shock and expansion tunnel facilities. Through the works of Petrie-Repar [13] and Johnston [10], a moving mesh capability was added. This functionality was first exercised by Qin *et al.* for comparatively low speed FSI when investigating the flexible top foils in bump–type foil bearings [15] and has been used for shock-fitting capabilities by by Damm [7]. T These already implemented features make Eilmer well suited for the analysis of hypersonic FSI problems.

The aim of the current paper is to report on the implementation of a FEM solver within the Eilmer CFD software package that facilitates full two-way coupling, while maintaining a high computation speed to enable time-accurate solutions.

Test Piece, Data, and Operating Conditions

The test geometry used in the current study is based on the model HyFoil0.3, that was first designed by Currao and is reported in Currao *et al.* [6]. While the actual model is three-dimensional, the model was designed with a width of 80 mm to minimise edge-effects and to ensure span–wise pressure uniformity and a two-dimensional structural behaviour. This makes the model and data well suited for comparison to 2-D simulations. The model was manufactured from Al-6061-T6 and consisted of a rigid support with a flexible tail as shown in figure 1. During the experiment, the support remained rigid and only the 2 mm thick flexible plate responds to the flow.

Parameter	Value	Parameter	Value
Length (mm)	130	Thickness (mm)	2 (1.95)
E (GPa)	52.7	Density (kg m^{-3})	2668
ζ (-)	0.0038	$R_{leading\,edge}$ (mm)	0.5

Table 1: Model dimensions and mechanical properties [6].

Parameter	Value	Parameter	Value
$P_{initial}$ (Pa)	50	$T_{initial}$ (K)	290
P_{static} (Pa)	755	T_{static} (K)	75
P_{total} (Pa)	968×10^3	T_{wall} (K)	300
M_∞ (-)	5.8	U_∞ (m s^{-1})	1006.8

Table 2: Initial and inflow conditions, adapted from [6].

The geometric and mechanical properties of the flexible plate are summarised in table 1. Young's modulus (E) and damping ratio (ζ) are experimentally determined values, measured from the actual test hardware. Concerning the plate thickness, the measured value is 1.95 mm, while the nominal value of 2.0 mm is employed across the current simulations.

Experimental data used for verification of the simulations was collected in the free-piston compression-heated Ludwieg tube (TUSQ) at the University of Southern Queensland [4] and presented by Currao *et al.* [6]. The model, initially at rest, experienced the start-up of the tunnel flow. The flow stabilised in few milliseconds, and the resultant pressure difference between the windward and leeward side of the flexible plate was sufficient to initialise a dynamic response. Similar experiments were conducted by Yamada *et al.* and Buttsworth *et al.* to investigate the response of rigid structures [20, 3]. The fluid conditions prior to flow arrival (initial) and once the flow has established are summarised in table 2.

Simulation Set-up

The two-way coupled simulations are achieved by implementing the coupling approach schematically shown in figure 2. First, the flow solution is interrogated to extract the pressure acting on the flexible portion of the model. Next, these nodal forces are employed in the FEM solver. Structural displacement and velocity are then retrieved and used to update the mesh, in order to ensure that the fluid domain remains conformant to the boundary conditions. Finally, the fluid dynamic conservation equations are solved on the moving mesh, and the solution is fed back to the FEM solver at the next coupling step.

To accelerate the solution process it is possible to sub-cycle the fluid-dynamic solver, thereby reducing the computational costs from the structural solver and the computational overheads arising from updating the mesh velocity. Numerical studies by Trudgian [18] showed that this approach yields results independent of mesh motion update interval, as long as the movement between two updates is less than half a cell height. In the current work, both fluid and structure solver are updated with the same time-step as determined from the CFL criterion set by the fluid solver.

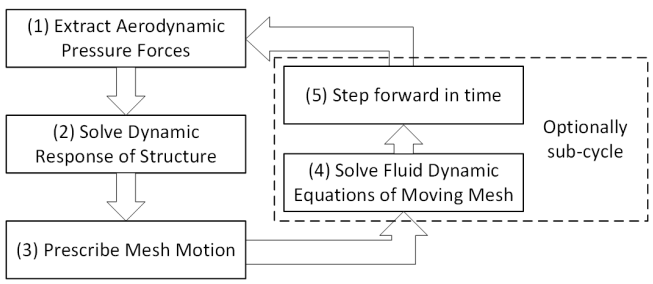

Figure 2: Implementation of two-way coupling.

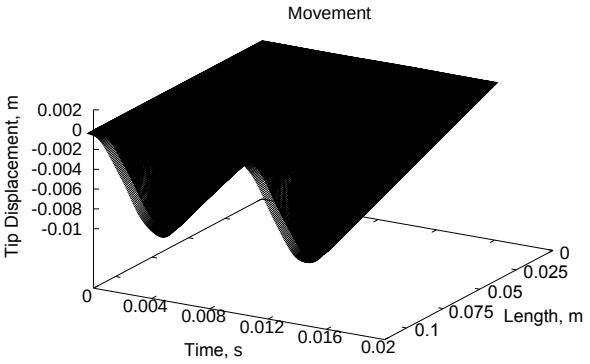

Figure 3: Movement history for flexible plate.

The following sections describe the implementation of the different steps.

(1) Force Extraction

For the current study fluid mesh vertices and structural nodes are colocated. This allows pressures at cell centres to be extracted and applied as distributed loads to the corresponding structural elements. In the same way, it is possible to extract wall shear stress, which can be applied as a distributed shear force on the corresponding structural element.

(2) Finite Element Model

To obtain the dynamic response, a FEM model, based on a 2D linear Euler–Bernoulli beam model is employed:

$$D\frac{\partial^4 w}{\partial x^4} = p(x,t) - \mu\frac{\partial^2 w}{\partial t^2} \tag{1}$$

where, $D = EI/(1-\nu^2)$ is the flexural rigidity, μ is the mass per unit length and p is the net aerodynamic pressure. The structural displacement w of a beam element can be written as:

$$w(x,t) = N_j(x)w_j(t), \quad j = 1,2 \tag{2}$$

where $\mathbf{N}(\mathbf{x})$ is the shape function vector and $\mathbf{w}(t) = [w_1\,\theta_1\,w_2\,\theta_2]^T$ is the nodal vector of the beam element. The model neglects in–plane deformation. It can be demonstrated that this assumption is generally appropriate for a cantilevered plate, which does not undergo measurable longitudinal deformations in this experiment. For the same reason, deformation contributions arising from viscous shear forces acting on the plate are ignored. A large-deflection model is not required to accurately resolve the oscillatory motion of the plate [6]. This is due to both the cantilevered configuration and the fact that trailing-edge displacement history presents a maximum amplitude of 5 plate thicknesses. For a single beam element, the dynamic FEM model can be written as:

$$M\ddot{\mathbf{w}} + \tilde{D}\dot{\mathbf{w}} + K\mathbf{w} = \mathbf{f} \tag{3}$$

where M, $\tilde{D}$ and K are the mass, damping and stiffness matrix; $\mathbf{f}$ is the load vector retrieved from the fluid solver. The problem can be rewritten as $\dot{y} = f(t,y)$ with $y = [\mathbf{w}\,\dot{\mathbf{w}}]^{\mathbf{T}}$. The equation is then solved using explicit forward time stepping:

$$y^{n+1} = y^n + f(t,y) \tag{4}$$

with a time step $\Delta t = t^{n+1} - t^n$ of approximately 10×10^{-6} s for a 26 element beam. The explicit time-stepping has been

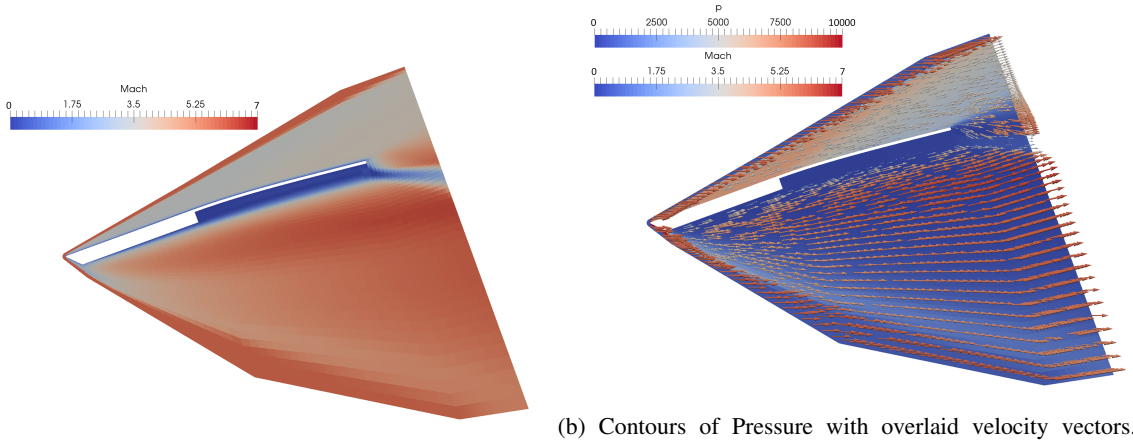

(a) Contours of Mach number.

(b) Contours of Pressure with overlaid velocity vectors. (Pressure values capped at 10 kPa)

Figure 4: Snap-shot of unsteady pressure and Mach distribution at time $t = 5$ ms.

compared to a 4th order Runge–Kutta method and, for current problem and time-step, the differences are negligible.

(3) Mesh Motion

For the solution of the fluid dynamic governing equations on the moving mesh, the fluid solver requires the position and velocities of all the vertices in the mesh. The boundary velocities along the top and bottom of the flexible plate are available directly from the first derivative of the beam element nodal vector, $\dot{\mathbf{w}}$. For the portions of the mesh above and below the beam the vertex velocities are prescribed by linearly scaling the mesh velocity with respect to distance from the flexible plate, so that the corresponding vertices at the far-field boundary remain stationary. The mesh downstream of the trailing edge follows the trailing edge motion, but does not move in the axial direction.

(4) Fluid Solver

The fluid dynamic simulations are conducted using the finite volume CFD code Eilmer [9]. The solver uses the finite volume formulation and is based on the AUSMV family of flux calculators [19]. By default, it is second–order accurate in space and time. In the proximity of strong shocks the Equilibrium Flux Method (EFM) scheme [11, 14] is used to increase numerical diffusion and to ensure stability. The solver has undergone extensive verification and validation [8] and has been the work-horse for time-accurate expansion tunnel simulations at the Centre for Hypersonics at the University of Queensland.

For fluid simulations involving moving boundaries it uses a boundary conforming moving mesh implementation [10]. This means that when solving the fluid dynamic governing equations, the interface velocity w_{if} is incorporated in the calculation of inviscid fluxes. The resulting convective flux vector becomes:

$$\mathbf{F}'_i = \begin{bmatrix} G' \\ L' \\ H' \end{bmatrix} = \begin{bmatrix} \rho\,(\mathbf{u} - w_{if}) \cdot \hat{\mathbf{n}} \\ \rho\,(\mathbf{u} - w_{if})\,(\mathbf{u} - w_{if}) \cdot \hat{\mathbf{n}} + p\,\hat{\mathbf{n}} \\ \rho E\,(\mathbf{u} - w_{if}) \cdot \hat{\mathbf{n}} + p\,(\mathbf{u} - w_{if}) \cdot \hat{\mathbf{n}} \end{bmatrix} \quad (5)$$

where G', L', and H' are the mass, momentum and energy fluxes relative to the moving mesh. The critical step in this approach is the calculation of the interface velocity, w_{if}, which must be set to ensure the geometric conservation law is satisfied. This is achieved by using the concept of a face velocity analogous to the edge velocity proposed by Ambrosi *et al.* [1].

Viscous fluxes are calculated after the mesh has moved and do not consider movement of vertices directly. However, along wall boundaries the wall motion acting on the fluid in the cell must be considered. This is achieved by calculating a representative wall velocity, equal to the average of corresponding vertex velocities and using this for the viscous flux calculation. The work done on the fluid due to wall movement in the wall normal direction is accounted for by an extra source term.

(5) Time Update

The time–step for the fluid update is governed by the stability (CFL) criterion imposed by the fluid solver. A time-step of 1×10^{-8} s is maintained for the current simulations, which ensures a CFL number of less than 0.5, implying a time-accurate solution.

Performance

For the current proof-of-concept simulations the fluid domain consisted of 7660 cells and the flexible portion of the plate is discretised using 26 beam elements. Using 10 cores on a cluster we can time-march for approximately 11.5 ms simulation time for every 24 h wall clock time. Substantial acceleration is expected through further parallelisation and the use of sub-cycling as illustrated in figure 2.

Discussion

The plate deflection results for the first 16 ms of the simulation, corresponding to approximately one-and-half oscillations are shown in figure 3. The motion generally resembles the response of a beam subjected to a step increase in pressures. The pressure and Mach number contours at time, $t = 5$ ms, which correspond to the maximum structural deflection shown in figure 4. To minimise computational cost for the FSI simulations, the fluid domain starts just upstream of the leading edge shock. For the current proof-of-concept simulations the mesh is too coarse to accurately resolve the boundary layer, nevertheless the formation of a slow–moving fluid–layer in the first cell is evident in figure 4a. Validation of the simulation is possible through comparison against experimental pressure measurements performed by Currao *et al.* [6]. In the present work, pressures on the leeside of the flexible plate increases from 80 to 136 Pa, thus comparable to the measured data (122 ± 30) Pa. Pressure in the vicinity of the pressure transducer located at 215 mm from plate leading edge on the windward side exceeds, 6600 Pa, the measured pressure is approximately 6000 Pa. This is probably due to transient effects and initial pressure non-unifomity associated with tunnel start-up, which are not modelled in the current simulation. The amplitude of pressure fluctuations is approximately 2600 Pa, which is in close agreement with the experimental measurements.

To gain an understanding of the coupled response, figure 5 shows the motion history for plate tip from the current simula-

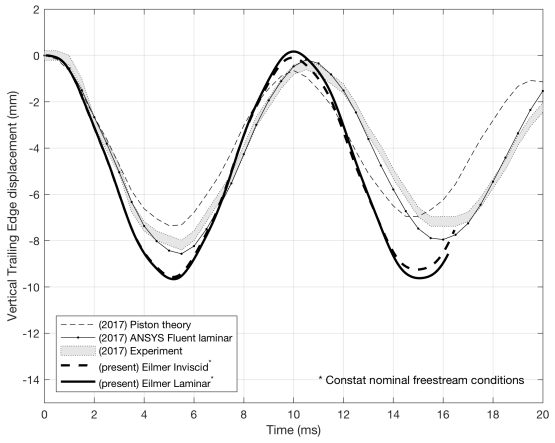

Figure 5: Comparison of plate tip deflection to experimental data and previous simulations reproduced from [6]

tions, experimental data, and previous numeric studies. Deflection amplitudes are over-predicted by approximately 20 %. This can be explained by the higher windward side pressure observed in the current simulations, but further investigation is required. The period of the oscillations is slightly shorter than the experiments and in closer agreement with the Piston theory results. Considering that both approaches use the same Euler-Bernoulli beam model, this is expected.

Future Work

The current work has demonstrates the ability to conduct two–way coupled FSI simulations by implementing a FEM solver as part of Eilmer. To continue this work we will seek ways to improve the computational efficiency of this approach, to solve more complex and larger problems. Planned improvements include, advanced structural models, increased parallelisation, and addition of shock–fitting capabilities.

Conclusions

Through implementing a FEM solver as part of the Eilmer CFD solver we have demonstrated the ability to conduct *fast* two–way (strong) coupled FSI simulations for hypersonic flows. The current work has concentrated on a flexible cantilevered plate which is modelled as a Euler–Bernoulli beam. We show that predictions with Eilmer are in broad agreement with experimental data and previous numerical studies. Using the time–accurate solution process of the fluid dynamic equations implemented in Eilmer provides us with a tool for detailed investigations of the underlying physics that drive high speed FSI.

Acknowledgements

Aspects of this research were supported by AFOSR under Grant FA2386-16-1-4024. This work was also supported by the Australian Research Council under grant ARC-DP180103480.

References

[1] Ambrosi, D., Gasparini, L. and Vigevano, L., Full potential and euler solutions for transonic unsteady flow, *The Aeronautical Journal*, **98**, 1994, 340–348.

[2] Bowcutt, L., Paull, A., Dolvin, D. and Smart, M., Hifire: An international collaboration to advance the science and technology of hypersonic flight, *28th International Congress of the Aeronautical Sciences*.

[3] Buttsworth, D., Stern, N. and Choudhury, R., A demonstration of hypersonic pitching control in the tusq hypersonic wind tunnel, *55th AIAA Aerospace Sciences Meeting, AIAA SciTech Forum*.

[4] Buttsworth, D. R., Ludwieg tunnel facility with free piston compression heating for supersonic and hypersonic testing, *9th Australian Space Science Conference*, 153–162.

[5] Currao, G. M. D., Neely, A. J., Buttsworth, D. R. and Choudhury, R., Measurement and simulation of hypersonic fluid-structural interaction on a cantilevered plate in mach 6 flow, *AIAA SciTech Forum*, 1–16.

[6] Currao, G. M. D., Neely, A. J., Buttsworth, D. R. and Gai, S. L., Hypersonic fluid-structure interaction on a cantilevered plate., *7th European Conference for Aeronautics and Space Sciences (EUCASS)*.

[7] Damm, K., Shock fitting mode for Eilmer., SoMME Technical Report 2016/15, The University of Queensland, Brisbane, Australia, 2016.

[8] Gollan, R. J. and Jacobs, P. A., About the formulation, verification and validation of the hypersonic flow solver Eilmer., *International Journal for Numerical Methods in Fluids*, **73**, 2013, 19–57.

[9] Jacobs, P. and Gollan, R., Implementation of a compressible-flow simulation code in the D programming language, 2016, volume 846 of *Applied Mechanics and Materials*.

[10] Johnston, I., Simulation of flow around hypersonic blunt-nosed vehicles for the calibration of air data systems, Phd thesis, University of Queensland, Mechanical Engineering, 1999.

[11] Macrossan, M. N., The equilibrium flux method for the calculation of flows with non-equilibrium chemical reactions., *Journal of Computational Physics*, **80**, 1989, 204–231.

[12] McNamara, J. and Friedmann, P., Aeroelastic and aerothermoelastic analysis in hypersonic flow: past, present, and future, *AIAA Journal*, **49**, 2011, 1089–1122.

[13] Petrie-Repar, P., Numerical simulation of diaphragm rupture, Phd thesis, University of Queensland, Mechanical Engineering, 1997.

[14] Pullin, D. I., Direct simulation methods for compressible inviscid ideal-gas flow., *Journal of Computational Physics*, **34**, 1980, 231–244.

[15] Qin, K., Jahn, I.H.J. ; Gollan, R. and Jacobs, P., Development of a computational tool to simulate foil bearings for supercritical co2 cycles., *Journal of Engineering for Gas Turbines and Power*, **138**.

[16] Riley, Z. and McNamara, J., Interaction between aerothermally compliant structures and boundary layer transition in hypersonic flow, *AIAA SciTech Forum*, 3–9.

[17] Riley, Z., McNamara, J. and Johnson, H., Assessing hypersonic boundary-layer stability in the presence of structural deformation, *AIAA Journal*, **52**, 2014, 2548–2556.

[18] Trudgian, M., Modelling of the hypersonic flow around an actuator using a dynamic mesh., BEng Thesis, The University of Queensland, 2014.

[19] Wada, Y. and Liou, M. S., A flux splitting scheme with high-resolution and robustness for discontinuities., AIAA Paper 94-0083, 1994.

[20] Yamada, K., Jahn, I. and Buttsworth, D., Experimental and analytical investigation of hypersonic fluid-structure-interactions on a pitching flat plate airfoil, 2016, volume 846 of *Applied Mechanics and Materials*.

[21] Zuchowski, B., Predictive capability for hypersonic structural response and life prediction: Phase ii - detailed design of hypersonic cruise vehicle hot-structure, Final Report AFRL-RQ-WP-TR-2012-0280, Air Force Research Laboratory, 2012.